Optical Switching and Networking 28 (2018) 8–22

Contents lists available at ScienceDirect

Optical Switching and Networking

journal homepage: www.elsevier.com/locate/osn

FiWi network throughput-delay modeling with traffic intensity control and local bandwidth allocation

Po-Yen Chen, Martin Reisslein*

School of Electrical, Computer, and Energy Engineering, Arizona State University, Tempe, AZ 85287-5706, United States

ARTICLE INFO

Keywords:
Fiber-Wireless (FiWi) network
Input traffic rate control
M/M/1/K queue
Node level design
Poisson traffic
Throughput-delay analysis

ABSTRACT

Fiber-Wireless (FiWi) networks typically combine an optical access network with a wireless access network so as to build on the respective strengths of the optical and wireless network technologies. Prior analytical throughput-delay studies of FiWi networks have typically considered heavy-loaded traffic models, i.e., constantly backlogged source nodes. In contrast, in this paper we present a more general comprehensive FiWi network throughput-delay analysis that encompasses Poisson (non-heavy) as well as heavy-loaded input traffic models. In addition, our analysis covers bandwidth assignments of wireless channels both at the hop distance level and at the node level, as well as a queuing model of dynamic bandwidth allocation in the optical access network. Our analysis provides insightful guidelines for setting the channel access probabilities for source traffic and relay traffic in FiWi networks. Our numerical evaluations demonstrate that prior studies which considered only heavy traffic loads gave misleading results for the delay performance of well-known access probability assignments. We correct and clarify these misleading results with our more general analysis for non-heavy traffic.

1. Introduction

A Fiber-Wireless (FiWi) network typically provides a high-speed optical backhaul network for a wireless mesh network (WMN) [1–6]. The optical backhaul network of a FiWi network is usually based on a passive optical network (PON) [7–16], whereby distributed Optical Network Units (ONUs) serve as backhaul gateways for clusters of WMN nodes. A fundamental design challenge in FiWi networks is to assign the WMN channel access opportunities to the different WMN nodes so as to enable efficient forwarding of the WMN traffic towards the ONUs for transmission to the central Optical Line Terminal (OLT) of the PON. In particular, each WMN node m_i needs to be assigned a probability p_i for channel access, and a probability q_i for forwarding relay traffic (rather than transmitting its own source traffic within a given channel access opportunity). As reviewed in Section 2, prior research, e.g., [17,18], has studied these probability assignments and the resulting FiWi network throughput-delay performance for heavy-loaded traffic where all nodes are constantly backlogged. The heavy-loaded traffic model simplifies analysis and is commonly considered in order to make complex network models analytically tractable. With the heavy-loaded traffic model, source queues are constantly backlogged and are able to transmit a packet whenever offered a transmission opportunity. This prior research found that expediting the forwarding of relay packets, i.e., setting very high forwarding probabilities q_i, reduces mean packet delays.

In contrast, we analyze the FiWi network for a non-heavy Poisson traffic model. This non-heavy traffic model enables us to consider the queueing delays at the original source nodes, which were ignored in the prior heavy-traffic model studies. We find that our more general FiWi network model accommodating non-heavy Poisson traffic and the source node queueing delays leads to fundamentally different conclusions about the forwarding probability setting. In contrast to the heavy-traffic studies, such as [17,18], we find that expediting the forwarding of relay packets does *not* reduce the mean packet delay. Instead, we introduce (*i*) an input traffic control strategy as well as (*ii*) a novel channel access and forwarding probability design strategy based on the traffic characteristics at the individual nodes to effectively reduce the mean packet delay.

This article is organized as follows. Section 2 reviews related FiWi network research. Section 3 presents the FiWi network model, including the non-heavy Poisson traffic model and the queuing structure in the FiWi network nodes. Section 4 gives the mathematical FiWi network throughput-delay analysis. Section 5 introduces the input traffic control strategy as well as the node based transmission and forwarding probability design. Section 6 presents numerical results based on the mathematical analysis and verifying simulations. Section 7 summarizes the conclusion of this FiWi network analysis study.

* Corresponding author.
E-mail addresses: pchen45@asu.edu (P.-Y. Chen), reisslein@asu.edu (M. Reisslein).

https://doi.org/10.1016/j.osn.2017.11.001
Received 22 March 2017; Received in revised form 4 October 2017; Accepted 2 November 2017
Available online 03 November 2017

2. Related work

A seminal line of WMN research found that backhauling with wire-connected gateways, i.e., a hybrid two-tiered network structure consisting of wireless nodes and wired gateways, can increase the network throughput [19–22]. This line of research focused primarily on asymptotic analyses for a number of nodes growing to infinity and has limited direct applicability for FiWi networks with a finite number of nodes.

Another line of related research has developed queuing models for specific aspects of WMNs. For instance, specific tree topologies have been examined in [23,24]; whereas we consider arbitrary topologies. An $M/D/1$ queueing model for scheduling on individual WMN links has been developed by Naeini [25]. Chen et al. [26] modeled each WMN node as a single queue; whereas we model each WMN node as a combination of two $M/M/1/K$ queues so as to distinguish the queueing of locally generated source traffic and the queueing of relay traffic. Pandey et al. [27] analyzed the impact of a specific load balancing approach on the gateway nodes, which were modeled with $M/M/1$ queues. In contrast, we develop a more comprehensive queueing model encompassing all the WMN nodes and gateways (ONUs).

Most prior analytical WMN and FiWi studies have considered the heavy-loaded traffic model, e.g., [17,18,28,29]. Relatively few analytical studies that are complementary to our study have considered non-heavy Poisson traffic. Bisnik and Abouzeid [30] have developed a queueing diffusion approximation model that considers random walk packet routing for non-heavy traffic. In contrast, we consider fixed routing along a prescribed path, e.g., the shortest path to the gateway. Wang et al. [31] have developed a game-theoretic model of the medium access control (MAC) protocol for non-heavy traffic that optimizes the transmission power level; the routing paths enabled by the optimized transmission power could be considered in our FiWi network model.

FiWi network routing and scheduling mechanisms have been proposed in [32–37]. FiWi network throughput-delay analyses that are complementary to our study by focusing on specific MAC and quality of service mechanisms have been conducted in [38–44]. Studies on energy saving mechanisms and their impact on FiWi network performance have been presented in [45–51]. The present study contributes an original fundamental FiWi network throughput-delay analysis that accommodates non-heavy Poisson traffic. Our analysis provides a basis for studying the interactions between clusters of WMN nodes and the PON backhaul.

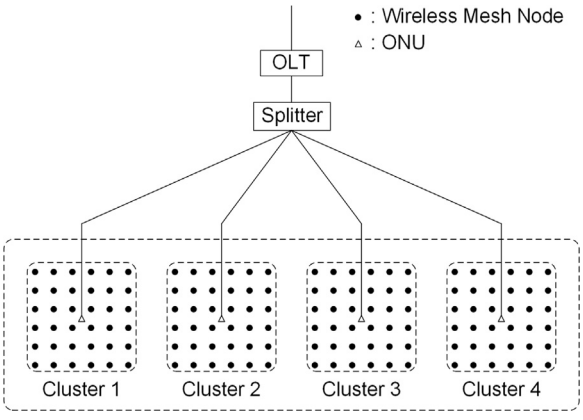

Fig. 1. FiWi network architecture example: The original wireless mesh network (WMN) is partitioned into $Z = 4$ clusters. Each cluster is served by an optical network unit (ONU) of the passive optical network (PON).

3. FiWi network model

3.1. Network architecture

A FiWi network is formed by partitioning the original wireless mesh network (WMN) into Z non-overlapping clusters, as illustrated for $Z = 4$ in Fig. 1. Each cluster is served by one ONU. We focus on static clustering in this study. We note that for $Z = 1$, the FiWi network is identical to the original WMN. Within each cluster, packets are forwarded in multihop fashion to the cluster's ONU (gateway). Throughout, we assume that all wireless transmissions are conducted in the same radio frequency band with a transmission bit rate W [bit/s], and transmission range r [m]. An upstream packet that has reached the ONU is placed in a queue to await transmission out of the WMN to the OLT.

3.2. Traffic model

We consider the locally generated traffic at a given wireless mesh node m_i to follow a Poisson process with rate $\lambda_{s,i}$. That is, the time period between the generation of two successive source traffic packets at node m_i has an exponential distribution with mean $1/\lambda_{s,i}$.

3.3. Node model: Source and relay queues

We model a given WMN node m_i, $i = 1, \ldots, N$, with two queues: the source queue Q_s serves the locally generated (source) packets, while the relay queue Q_r serves the relayed packets, as illustrated in Fig. 2. In particular, the two queues in WMN node m_i are served as follows:

1) If Q_r and Q_s are not empty, transmit a packet from Q_r with probability q_i, or a packet from Q_s with probability $1 - q_i$.
2) If Q_r is empty and Q_s is not empty, transmit a packet from Q_s.
3) If Q_s is empty and Q_r is not empty, transmit a packet from Q_r.
4) If Q_r and Q_s are both empty, do nothing.

Note that a heavy traffic model would simplify the forwarding model in that the source queue Q_s would never be empty; in contrast, we consider a non-heavy traffic model, where the source queue Q_s may be empty. We do not consider adaptive bandwidth sharing among WMN nodes in the packet forwarding model. In particular, if a transmission opportunity is given to a WMN node with empty Q_r and Q_s, the transmission opportunity is wasted. The analysis of adaptive bandwidth sharing is left for future research. Studies [18,17] demonstrated that heavy-loaded traffic, which assumes that the source queues are always full, avoids wasted transmission opportunities. However, the service models for heavy-loaded traffic do not directly consider the delays in the source queues. Network designs that consider the source traffic delays are introduced in Section 5.

3.4. Routing protocol

Shortest path routing (i.e., minimum hop count routing) is employed within each WMN cluster. Nodes with multiple next-hop candidates (along the shortest path route) randomly select one of them on a per-packet basis. As is common for WMNs [52,53], we assume that each cluster is highly connected and each WMN node has at least

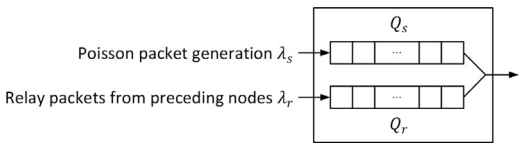

Fig. 2. Model of a WMN node: Source queue Q_s serves locally generated packets; whereas relay queue Q_r forwards packets from other nodes.

one path to its corresponding gateway (ONU). We define an x-hop node as a WMN node with hop distance x to its corresponding gateway.

3.5. Medium access control protocol

3.5.1. WMN

We consider a generic WMN MAC model [18], which characterizes the WMN behavior through the probability p_i of successful channel access. In particular, node m_i obtains the transmission opportunity of a given time slot (with duration t_c, i.e., for a single packet transmission) of a time-division-multiplexing-access (TDMA) system with probability p_i. Many factors influence the WMN channel access probability p_i, including physical channel conditions and interference from neighboring nodes as well as scheduling policies and MAC protocols [54]. The set of probabilities p_i characterizing a specific WMN can be obtained through measurements. Generally, nodes m_i with shorter hop distances to the gateway should be assigned higher probabilities p_i since transmission opportunities a node m_i are consumed by both relayed and locally generated traffic, whereby nodes closer to the gateways experience typically higher relay traffic loads. In this paper, we study the effects of p_i designs that are based on the hop distance as well as designs based on individual nodes.

3.5.2. PON

We suppose that all gateways (ONUs) are identical and provide packet forwarding service to the OLT. The ONUs transmit the received packets to the OLT with a direct optical transmission (i.e., with one optical transmission hop). The ONU packet transmissions are controlled through a MAC protocol executed by the central OLT, whereby typically several packets are grouped together for an upstream transmission from an ONU to the OLT. We consider a constant transmission bitrate scenario, where we model the ONUs as $M/D/1/K$ queues, see Section 4.7.1. We also consider a scenario with dynamic sharing of the optical transmission bitrate among the ONUs through dynamic bandwidth allocation (DBA). For the DBA scenario, we approximately model the ONUs as $M/M/1/K$ queues with different service rates, see Section 4.7.2.

4. Throughput and delay analysis

This section presents the mathematical FiWi network analysis. First, we analyze the queuing at a given WMN node m_i, followed by the derivation of the WMN delay and throughput. Based on the WMN results, we evaluate the PON delay and throughput. We analyze the overall FiWi network performance by combining the WMN and PON analyses. The main analysis notations are summarized in Table 1.

4.1. Packet service rates at WMN node m_i

Consider a TDMA system with time slot duration t_c and channel access probability p_i for node m_i in a given slot. Over a long time horizon, the arrival of transmission opportunities at node m_i can be approximately modeled as a Poisson process with rate $\mu_i \approx p_i/t_c$ [17,55]. The arrival rate μ_i of transmission opportunities to node m_i is equivalent to the service rate of packets at node m_i, whereby the service rate μ_i is shared by the local packet queue Q_s and the relay packet queue Q_r.

As noted in Section 3.3, the relay packet queue Q_r can obtain a given transmission opportunity that has been granted to node m_i under two circumstances: 1) The transmission opportunity is directly given to Q_r, and 2) the transmission opportunity is first given to the empty Q_s and then given back to Q_r. Thus, the service rate of the relay packet queue Q_r is

$$\mu_{r,i} = \mu_i q_i + \mu_i(1 - q_i)P_{0,s,i}, \tag{1}$$

where q_i is the probability of the transmission opportunity being given directly to Q_r, while $P_{0,s,i}$ is the probability of Q_s of m_i being empty [which can be obtained as $P_{M,0}(\rho_{s,i}, K)$ from Eq. (57)] and $(1 - q_i)P_{0,s,i}$ is the probability of the transmission opportunity first being given to the empty Q_s and then given back to Q_r. Note that the arrival of transmission opportunities to Q_r is a Poisson process since the arrival of transmission opportunities at Q_r is a proportion of the original Poisson process with rate μ_i. Similarly, we obtain the service rate of the local packet queue Q_s as

$$\mu_{s,i} = \mu_i(1 - q_i) + \mu_i q_i P_{0,r,i}, \tag{2}$$

where $P_{0,r,i}$ is the probability of Q_r of m_i being empty [obtained from Eq. (57)]. Similar to Q_r, the arrival of transmission opportunities at Q_s is a Poisson process.

Based on the service rates of Q_r and Q_s, we can further obtain the actual output rates of both queues:

$$\sigma_{r,i} = \mu_{r,i}(1 - P_{0,r,i}) \tag{3}$$

$$\sigma_{s,i} = \mu_{s,i}(1 - P_{0,s,i}). \tag{4}$$

Table 1
Summary of main notations.

Notation	Definition
Network structure	
m_i	Wireless mesh node i, $i = 1, \ldots, N$
H	Largest hop distance of the network
h_i	Hop distance from node m_i to the gateway (ONU)
$N(x)$	Number of nodes with hop distance x
S_x	$S_x = \{j: h_j = x \text{ for } j = 1, \ldots, N\}$ Set of indices of nodes with hop distance x
R_i	$R_i = \{j: m_i \text{ is a possible next hop of } m_j$ for $j = 1, \ldots, N\}$= Set of indices of possible previous hops of m_i
f_j	Number of possible next hops of node m_j
Z	Number of WMN clusters, indexed z, $z = 1, \ldots, Z$
C_z	$C_z = \{j: m_j \text{ is a 1-hop node in cluster } z$ for $j = 1, \ldots, N\}$= Set of indices of 1-hop nodes of cluster z
t_c	TDMA time slot duration=packet transm. time [s]
Channel access and forwarding prob.	
p_i	Channel access prob. of wireless mesh node m_i
q_i	Forwarding prob. of wireless mesh node m_i
Packet traffic rates at node m_i	
μ_i	$\mu_i = p_i/t_c$ Poisson process arrival rate of transmission opportunities at node m_i
$\lambda_{s,i}$	Source packet traffic generation rate
$\lambda_{r,i}$	Relay packet traffic arrival rate
$\mu_{s,i}$	Source packet traffic service rate
$\mu_{r,i}$	Relay packet traffic service rate
μ_i	Overall pkt. service rate, source + relay traffic
$\sigma_{s,i}$	Source packet traffic output rate
$\sigma_{r,i}$	Relay packet traffic output rate
$\rho_{s,i}$	Source packet traffic intensity at node m_i
$\rho_{r,i}$	Relay packet traffic intensity at node m_i
$M/M/1/K$ relay packet queue Q_r at WMN node m_i	
K	Buffer capacity in packets
$P_{b,r,i}$	Blocking prob. of relay queue Q_r at node m_i
$P_{0,r,i}$	Probability of Q_r being empty at m_i
$M/M/1/K$ source packet queue Q_s at WMN node m_i	
K	Buffer capacity in packets
$P_{b,s,i}$	Blocking prob. of source queue Q_s at node m_i
$P_{0,s,i}$	Probability of Q_s being empty at m_i
Throughput metric	
$T_W(x)$	Source packet traffic throughput of set of x-hop WMN nodes

The actual output rate of m_i, denoted as σ_i, is the sum of the output rates of its Q_r and Q_s. With (1), (2), and (3):

$$\sigma_i = \sigma_{r,i} + \sigma_{s,i} \tag{5}$$

$$= \mu_i(1 - P_{0,r,i} \cdot P_{0,s,i}). \tag{6}$$

Eq. (6) indicates that the transmission opportunities given to m_i are only wasted when both Q_r and Q_s are empty. This verifies the forwarding policy described in Section 3.3 and shows that the output traffic of node m_i is a Poisson process.

4.2. Packet arrival rates at WMN Node m_i

First we study the queuing behavior of the relay packet queue Q_r at WMN node m_i, followed by the local source packet queue Q_s at m_i. We define the set of possible preceding nodes of a given node m_i as $R_i = \{j: m_i \text{ is a possible next hop of } m_j, \text{ for } j = 1, \ldots, N\}$. The considered routing protocol (see Section 3.4) lets a given node select the next-hop node along the shortest path randomly among the possible next-hop candidates on a per-packet basis. Thus, the next-hop candidates equally share the outgoing traffic. In particular, let f_j denote the number of next-hop candidates of a preceding node m_j, $j \in R_i$ and note that σ_j/f_j is the input rate of relayed packets from the preceding node m_j to the relay packet queue Q_r of the considered node m_i. Hence, the relay packet arrival rate $\lambda_{r,i}$ at node m_i is

$$\lambda_{r,i} = \sum_{j \in R_i} \frac{\sigma_j}{f_j}. \tag{7}$$

The Poisson process properties of the packet flows ensure that the incoming and outgoing packet processes at the relay queue Q_r at m_i are Poisson processes. The relay packet queue Q_r of WMN node m_i can thus be modeled as an $M/M/1/K$ queue, with K denoting the buffer size in packets. We define the relay packet traffic intensity of Q_r at node m_i as

$$\rho_{r,i} = \frac{\lambda_{r,i}}{\mu_{r,i}}. \tag{8}$$

For the local source packet traffic queue Q_s of node m_i, we consider Poisson traffic with rate $\lambda_{s,i}$. Specifically, the distribution of the time span between two locally generated packets is exponentially distributed with mean $1/\lambda_{s,i}$. Since the arrival of transmission opportunities at Q_s is approximately a Poisson Process, see Section 4.1, the local source queue Q_s of node m_i can also be modeled as an $M/M/1/K$ queue. In particular, for the arrival rate $\lambda_{s,i}$ and service rate $\mu_{s,i}$, we define the source traffic intensity of Q_s at m_i as

$$\rho_{s,i} = \frac{\lambda_{s,i}}{\mu_{s,i}}. \tag{9}$$

4.3. $M/M/1/K$ Queue model for relay queue Q_r and local queue Q_s

As explained in Section 4.2, the relay queue Q_r and local source queue Q_s in a given WMN node m_i can be modeled as $M/M/1/K$ queues, which are briefly reviewed in the Appendix. For a fixed holding capacity of K packets, the mean waiting time $W_M(\mu, \lambda, K)$, see Eq. (59), is a function of both the service rate μ and the arrival rate λ. On the other hand, the probabilities of the queue being empty [$P_{M,0}$, see Eq. (57)] and full [$P_{M,K}$, see Eq. (56)] depend only on the traffic intensity ρ. Thus, the evaluation of the delay (average waiting time in the $M/M/1/K$ queue) in a given WMN node m_i requires the packet arrival and service rates at both Q_r and Q_s at WMN node m_i, as derived in Section 4.2.

4.4. Dynamic bandwidth adjustment at WMN nodes

In this subsection, we show that the bandwidth given to a WMN node m_i is dynamically adjusted if the input traffic is properly controlled. This property will be used in the input traffic control design proposed in Section 5.1 and in the channel access probability p_i design in Section 5.2. Let us consider the case that $\lambda_{r,i} < \mu_i q_i$, i.e., the incoming relay traffic rate is lower than the relay packet service rate [without considering the transmission opportunities given back to Q_r due to an empty Q_s, see Eq. (1)], and study the service rate of the local queue Q_s. With (1), (2), and (57), we obtain

$$\mu_{s,i} = \mu_i(1 - q_i) + \mu_i q_i P_{0,r,i} \tag{10}$$

$$= \mu_i(1 - q_i) + \mu_i q_i \frac{1 - \frac{\lambda_{r,i}}{\mu_i q_i + \mu_i(1 - q_i)P_{0,s,i}}}{1 - \left(\frac{\lambda_{r,i}}{\mu_i q_i + \mu_i(1 - q_i)P_{0,s,i}}\right)^{k+1}} \tag{11}$$

$$> \mu_i(1 - q_i) + \mu_i q_i \frac{1 - \frac{\lambda_{r,i}}{\mu_i q_i}}{1 - \left(\frac{\lambda_{r,i}}{\mu_i q_i}\right)^{k+1}} \tag{12}$$

$$> \mu_i(1 - q_i) + \mu_i q_i \left(1 - \frac{\lambda_{r,i}}{\mu_i q_i}\right) \tag{13}$$

$$= \mu_i - \lambda_{r,i}. \tag{14}$$

Thus, we have shown that if the incoming relay traffic rate $\lambda_{r,i}$ is lower than the lowest relay packet service rate $\mu_i q_i$, then the service rate $\mu_{s,i}$ of the local queue Q_s adjusts automatically to the lower incoming relay traffic rate and provides correspondingly higher service rate to the source packets, i.e.,

$$\mu_{s,i} > \mu_i - \lambda_{r,i} \quad \text{if} \quad \lambda_{r,i} < \mu_i q_i. \tag{15}$$

The analogous argument for the case $\lambda_{s,i} < \mu_i(1 - q_i)$ shows that

$$\mu_{r,i} > \mu_i - \lambda_{s,i} \quad \text{if} \quad \lambda_{s,i} < \mu_i(1 - q_i). \tag{16}$$

4.5. WMN throughput

The preceding Sections IV-B – IV-C, studied the incoming and outgoing packet traffic processes of a WMN node m_i. In particular, we showed that the relay packet queue Q_r and the local source packet queue Q_s in a WMN node m_i can be modeled as $M/M/1/K$ queues. An exact WMN analysis would require delay and throughput evaluations for all possible node-to-gateway paths for all WMN nodes. Such an exhaustive evaluation would become prohibitively complex for large WMNs where long hop distances lead to many possible paths to the gateway. We pursue therefore an approximate, low-complexity evaluation of the WMN throughput in this section, followed by an approximate delay analysis in Section 4.6.

First, we evaluate the end-to-end WMN throughput. For the set of x-hop WMN nodes, we define the local source packet traffic throughput $T_W(x)$ as the average number of packets generated by the x-hop WMN nodes that reach the gateways per unit time. Formally, $T_W(x)$ can be expressed as the total source packet traffic output rate of the x-hop nodes multiplied by the probability of the packets not being blocked at their local source nodes, nor at any of the intermediate relay nodes. Since the exhaustive evaluation of the blocking probabilities for all individual paths is prohibitive, we pursue the following approximate evaluation of the average blocking probability of the paths for the x-hop nodes. For the nodes with hop distance x, we first evaluate the weighted average relay packet blocking probability on the wireless WMN path as

$$P_{W,r,b}(x) = \frac{\sum_{i \in S_x} \lambda_{r,i} P_{M,K}(\rho_{r,i}, K)}{\sum_{i \in S_x} \lambda_{r,i}}, \tag{17}$$

where $S_x = \{i: h_j = x \text{ for } i = 1, \ldots, N\}$ is the set of x-hop nodes and $P_{M,K}(\rho_{r,i}, K)$ is obtained from Eq. (56). Similarly, we obtain the weighted average source packet blocking probability on the wireless WMN path for the nodes with hop distance x as $P_{W,s,b}(x)$ by replacing the subscript

r with the subscript s in Eq. (17).

All packets generated at x-hop nodes, with $x = 1, 2, \ldots, H$, have to pass through their source node and $x - 1$ relay nodes without blocking to reach the gateway. The aggregate throughput of the x-hop nodes can thus be evaluated as the product of the source packet traffic input rate of the x-hop nodes and the non-blocking probability. In particular, we define the aggregate source packet traffic output rate of the x-hop nodes as the product of the source packet traffic input rate of the x-hop nodes and the probability of not being blocked at the source node:

$$\sigma_{s,\text{agg}}(x) = \sum_{i \in S_x} \sigma_{s,i} = \sum_{i \in S_x} \lambda_{s,i}[1 - P_{\text{W},s,b}(x)]. \tag{18}$$

Nodes with $x = 1$ hop to the gateway cannot be blocked at a relay node, while nodes with $x = 2, 3, \ldots, H$ hops need to be relayed by $x - 1$ nodes without blocking to reach the gateway. Hence, the source packet traffic throughput of x-hop nodes for $x = 1, 2, \ldots, H$ is

$$T_{\text{W}}(x) = \begin{cases} \sigma_{s,\text{agg}}(1), & x = 1 \\ \sigma_{s,\text{agg}}(x) \prod_{h=1}^{x-1} [1 - P_{\text{W},r,b}(h)], & x = 2, \ldots, H. \end{cases} \tag{19}$$

Note that source traffic output rate $\sigma_{s,i}$ and blocking probabilities $P_{\text{W},s,b}(x)$ and $P_{\text{W},r,b}(x)$ are functions of channel access probability p_i and forwarding probability q_i; thus, the throughput depends on both p_i and q_i, as numerically evaluated in Section 6. We obtain the aggregate WMN throughput by summing $T_{\text{W}}(x)$ over the hop distance x:

$$T_{\text{W,agg}} = \sum_{x=1}^{H} T_{\text{W}}(x). \tag{20}$$

4.6. WMN delay

Based on the traffic rates at the individual wireless mesh nodes m_i evaluated in the preceding subsections, we derive in this subsection the mean WMN delays by considering the individual heterogeneous traffic loads at the WMN nodes. We define the end-to-end WMN delay of a newly generated packet as the time period from the time instant when the packet is placed in the local queue of the source node to the time instant when the last bit of the packet reaches the gateway. For a packet generated at an x-hop node, the end-to-end delay consists of the queuing delay at its source node, the queuing delays at the $x - 1$ intermediate nodes that relay the packet, and the length of the x time slots for the packet transmissions.

We approximate the average waiting time for the relayed packets in the relay queue Q_r of an x-hop node as

$$W_{\text{W},r,\text{avg}}(x) = \frac{\sum_{i \in S_x} \sigma_{r,i} W_{\text{M}}(\mu_{r,i}, \lambda_{r,i}, K)}{\sum_{i \in S_x} \sigma_{r,i}}, \tag{21}$$

whereby the mean waiting time $W_{\text{M}}(\mu_i, \lambda_i, K)$ is obtained from Eq. (59). Similarly, we obtain the average waiting time for the source packets in local queue Q_s of an x-hop node $W_{\text{W},s,\text{avg}}(x)$, which corresponds to Eq. (21) with subscript r replaced by subscript s.

Based on the average relay packet waiting time $W_{\text{W},r,\text{avg}}(x)$ and the average source packet waiting time $W_{\text{W},s,\text{avg}}(x)$ in a given WMN node with hop distance x, we evaluate the average end-to-end WMN delay as follows. A node with a hop distance $x = 1$ transmits a source packet to the gateway node when the transmission opportunity is granted to its Q_s. With the delay measurement starting at the time instant when a newly generated packet is placed in the local source queue Q_s, the source packet traffic generated at 1-hop nodes experiences an end-to-end WMN delay corresponding to its queuing delay at the local source queue Q_s plus the transmission delay t_c. Source packet traffic generated at x-hop nodes with $x = 2, 3, \ldots, H$, needs to be queued in the source queue Q_s and then transmitted x times and incurs the total queue waiting time corresponding to the source node and the relay nodes that are $1, 2, \ldots, x - 1$ hops from the gateway. In summary,

$$D_{\text{W}}(x) = \begin{cases} t_c + W_{\text{W},s,\text{avg}}(x) & \text{if} x = 1 \\ xt_c + W_{\text{W},s,\text{avg}}(x) & \\ \quad + \sum_{h=1}^{x-1} W_{\text{W},r,\text{avg}}(h) & \text{if} x = 2, \ldots, H. \end{cases} \tag{22}$$

We evaluate the average WMN end-to-end delay $D_{\text{W,avg}}$ by averaging the delays of packets reaching the gateways. In particular, we weigh the delay $D_{\text{W}}(x)$ experienced by x-hop nodes by the corresponding source traffic output rate $T_{\text{W}}(x)$ of x-hop nodes:

$$D_{\text{W,avg}} = \frac{\sum_{x=1}^{H} T_{\text{W}}(x) D_{\text{W}}(x)}{T_{\text{W,agg}}}. \tag{23}$$

4.7. PON throughput-delay analysis

When a packet reaches a gateway, the packet is immediately forwarded to the ONU operating at the gateway. Each ONU operates as a queue that transmits the queued packets to the OLT. All ONUs share the same physical optical transmission bitrate and several packet scheduling techniques have been proposed to efficiently control the bandwidth sharing [56–59]. In this paper, we consider both a basic model without any specific scheduling policy and a model with a basic dynamic bandwidth allocation (DBA) policy.

4.7.1. PON with fixed service rates

First we study the scenario where no DBA is applied. We suppose that the PON operates with TDMA such that each ONU can transmit its packets during specific time slots. This model results in a deterministic ONU service rate. Similar to the wireless TDMA network model, we denote t_{D} for the time slot duration needed to transmit a packet in the PON. We show that for this TDMA scenario, the ONUs can be modeled as $M/D/1/K$ queues, which allow for the derivation of the overall FiWi network delay and throughput.

For modeling the ONUs, we initially consider the packet arrival rates at the ONUs. Each ONU receives the packets directly from the corresponding WMN gateway, i.e., an ONU and its co-located gateway have the same input packet traffic characteristics. Let g_z, $z = 1, \ldots, Z$, denote the number of 1-hop nodes in cluster z. Analogously to the arguments in Section 4.2, the incoming packet process at each gateway is a Poisson process since it consists of the superposition of several Poisson processes. Therefore, the cluster z gateway receives the Poisson packet arrival rate

$$\lambda_{\text{D},z} = \sum_{j \in C_z} \sigma_j, \tag{24}$$

where C_z denotes the set of indices of the 1-hop nodes in cluster z. Since all Z ONUs operate with the same fixed rate (due to the static equal sharing of the total PON upstream transmission bitrate), each individual ONU can be modeled as an $M/D/1/K$ queue with service rate

$$\mu_{\text{D},z} = \frac{1}{t_{\text{D}} Z}. \tag{25}$$

The resulting ONU traffic intensity in cluster z is

$$\rho_{\text{D},z} = \lambda_{\text{D},z} t_{\text{D}} Z. \tag{26}$$

If a FiWi network serves both wireless users as well as wired users with direct connections to an ONU, e.g., through fiber to the home (FTTH), the ONU traffic load (intensity) is the sum of traffic loads from wireless and wired users.

We define the PON aggregate throughput $T_{\text{O,agg}}$ as the average number of packets reaching the OLT per unit time. The aggregate throughput $T_{\text{O,agg}}$ is the sum of the effective ONU output rates, i.e.,

$$T_{\text{O,agg}} = \sum_{z=1}^{Z} \lambda_{\text{D},z}[1 - P_{\text{D},K}(\rho_{\text{D},z}, K)], \tag{27}$$

where $1 - P_{D,K}(\rho_{D,z}, K)$ is the probability that the packets are not blocked. Clearly, the PON throughput is equivalent to the FiWi network throughput.

We obtain the average delay at the ONUs by weighing the delays $W_D(\mu_{D,z}, \lambda_{D,z}, K)$ at the individual ONUs z, $z = 1, \ldots, Z$, with the corresponding packet output rates $\lambda_{D,z}(1 - P_{D,K}(\rho_{D,z}, K))$:

$$W_O = \frac{\sum_{z=1}^{Z} W_D(\mu_{D,z}, \lambda_{D,z}, K)\lambda_{D,z}[1 - P_{D,K}(\rho_{D,z}, K)]}{T_{O,agg}}. \quad (28)$$

4.7.2. PON with dynamic bandwidth allocation

For the DBA schemes, each ONU includes a report message at the end of its upstream data packet transmission to signal the ONU queue length to the OLT as request for bandwidth for the next packet transmission cycle. After the OLT has received all ONU report messages, the OLT allocates the upstream transmission bitrate. Then, grant messages are sent to the ONUs indicating the transmission schedule for the next ONU upstream transmission cycle. Based on the report and grant messages, the optical bandwidth can be dynamically allocated and shared among all ONUs.

Let us consider the Gated DBA grant sizing scheme where the OLT grants the ONUs with sufficiently large transmission windows to transmit the entire reported queue length. With the Gated DBA, an ONU is capable of obtaining all the optical transmission bitrate which is not used by other ONUs. If the total WMN output rate is lower than the PON optical upstream transmission bitrate and each ONU is equipped with sufficiently large queues, we can expect the output rates of all ONUs to be the same as their input rates. We assume that the transmission bitrate consumed by the report and grant messages can be neglected and then based on the preceding observations, we model the service rate $\mu_{D,z}$ of a given ONU z as follows. Note that $1/t_D$ is the total available PON upstream transmission bitrate and that $\sum_{o=1,o\neq z}^{Z} \lambda_{D,o}$ is the optical bandwidth occupied by other ONUs $o \neq z$. Thus,

$$\mu_{D,z} = \frac{1}{t_D} - \sum_{o=1,o\neq z}^{Z} \lambda_{D,o}, \quad \text{if } \frac{1}{t_D} > \sum_{o=1,}^{Z} \lambda_{D,o}. \quad (29)$$

Eq. (29) indicates that a given ONU z can have higher service rates (than the equal share from Eq. (25)) if the other ONUs have lower input traffic, which is exactly the purpose of sharing through DBAs.

For saturation cases, where the total WMN output is higher than the PON upstream transmission bitrate, all the ONUs will eventually reach the state where the traffic intensities are greater than one. Since the ONUs with higher input traffic rates tend to request higher transmission bitrates, the optical transmission bitrate is shared among all ONUs in proportion to their input traffic rates whereby

$$\mu_{D,z} = \frac{1}{t_D}\frac{\lambda_{D,z}}{\sum_{o=1,}^{Z}\lambda_{D,o}}, \quad \text{if } \frac{1}{t_D} < \sum_{o=1,}^{Z} \lambda_{D,o}. \quad (30)$$

Similar to the non-DBA scenario in Section 4.7.1, the ONUs served with DBA have Poisson input traffic. However, the arrival of transmission opportunities at each ONU is random, but not Poisson (since the transmission opportunities arrive consecutively within the granted transmission window). Thus, the ONUs could be modeled as $M/G/1/K$ queues. However, the $M/G/1/K$ model requires the coefficient of variation of the service process, which is not readily available for the analysis. Hence, we chose to approximate the ONUs as $M/M/1/K$ queues with the service rates in Eqs. (29) and (30) since the traffic intensities and service rates are the primary determinant factors in the queuing analysis. Our numerical evaluations in Section 6.4 indicate that the $M/M/1/K$ queue approach provides a good approximation of the FiWi network performance.

4.8. FiWi network throughput and delay

The aggregate FiWi network throughput T_F is equal to the aggregate PON throughput as given by Eq. (27). Similar to the WMN analysis, we define the overall end-to-end delay of a packet in the FiWi network as the time period between the time instant when the newly generated packet is placed in the local source queue of the source node to the time instant when the last bit of the packet reaches the OLT. The FiWi network delay is the sum of the delays incurred at the WMN nodes and the ONUs. For packets generated at the x-hop nodes, the average delay is

$$D_F(x) = D_W(x) + W_O + t_D, \quad (31)$$

whereby t_D denotes the ONU transmission delay. The average end-to-end packet delay of a packet can be evaluated with the average WMN delay $D_{W,avg}$, see Eq. (23), and the average PON delay W_O, see Eq. (28), as

$$D_{F,avg} = D_{W,avg} + W_O + t_D. \quad (32)$$

5. Network design strategy

With heavy-loaded traffic, all transmission opportunities given to the WMN nodes are utilized, which gives the highest throughput of the network, but also only limited insights into the delay performance. In particular, with the heavy traffic model there is no notion of source queue Q_s delay; rather, with the heavy traffic model, the packet delay starts to be counted from the instant when the first bit of a packet is transmitted by the source node.

Based on the Poisson input traffic characteristics studied in the preceding sections, we propose 1) an input traffic control strategy for any given forward probability setting, and 2) a forward probability setting that can be used for both Poisson (non-heavy) and heavy-loaded input traffic.

5.1. Input traffic rate λ_s control strategy

We know from elementary queuing theory that the average queue size and the actual output rate increase when the input rate increases while the service rate remains fixed. As the input rate reaches the value where the traffic intensity $\rho > 1$, the actual output rate would be limited by the service rate and the average queue size increases rapidly until it approaches the value of K (i.e., the maximum number of packets that can be held in the queue). Section 4.4 also shows that the transmission opportunities given to a WMN node will be dynamically distributed between its local source and relay queues if the source or relay packet traffic flows do not exceed certain thresholds. Thus, for a given WMN node, the output rate can be maximized while maintaining a reasonable delay if the sum of the source and relay packet traffic rates is equal to the total packet service rate given to the node.

First, we propose a hop-wise design strategy, where the WMN nodes with the same hop distance have the same channel access probability, channel forward probability, and local input traffic rate:

$$p_i = p(x) \quad \forall \ i \text{ such that } h_i = x \quad (33)$$

$$q_i = q(x) \quad \forall \ i \text{ such that } h_i = x \quad (34)$$

$$\lambda_{s,i} = \lambda_s(x) \quad \forall \ i \text{ such that } h_i = x. \quad (35)$$

The hop-wise design strategy starts with edge nodes, i.e., the H-hop nodes, which have to serve only the source traffic. Our goal is to limit the total source traffic rate $N(H)\lambda_s(H)$ of the H-hop nodes to be lower than the total service rate $N(H)p(H)/t_c$ given to H-hop nodes, which results in the constraint

$$N(H)\lambda_s(H) \leq N(H)\frac{p(H)}{t_c}. \quad (36)$$

For the $H-1$ hop nodes, the total service rate $N(H-1)p(H-1)/t_c$ is available for the source packets and the relay packets from the H-hop nodes. The goal is also to limit the aggregate traffic rate resulting from the source packet rate $N(H-1)\lambda_s(H-1)$ of the $H-1$-hop nodes plus the relay traffic rate $N(H)\lambda_s(H)$ arriving form the H-hop nodes to be lower than the total service rate given to $H-1$-hop nodes, resulting in the constraint

$$N(H)\lambda_s(H) + N(H-1)\lambda_s(H-1) \leq N(H-1)\frac{p(H-1)}{t_c}. \tag{37}$$

Note that $N(H)\lambda_s(H)$ is indeed the maximum possible total relay traffic input rate form the H-hop nodes, which is also restricted to the maximum value $N(H)p(H)/t_c$ according to Eq. (36).

The analogous analysis can be applied to the following x-hop nodes where $1 \leq x \leq H$ and we can formulate the linear program for maximizing the aggregate input rate:

$$\text{Maximize} \quad \sum_{x=1}^{H} N(x)\lambda_s(x) \tag{38}$$

$$\text{Subject to} \quad \sum_{i=x}^{H} N(x)\lambda_s(x) \leq \frac{N(x)p(x)}{t_c}, \; x = 1, \ldots, H. \tag{39}$$

By maximizing the aggregate input rate while not violating the transmission bitrate restrictions, the linear program strives to maximize the system throughput while not constantly overflowing the buffers. If all WMN nodes have the same source traffic input rate, the solution of the linear program is

$$\lambda_{s,\text{opt}} = \min_{x=1,\ldots,H}\left[\frac{p(x)/t_c}{1+\sum_{i=x+1}^{H}\frac{N(i)}{N(x)}}\right]. \tag{40}$$

In a perfectly uniform network where all relay nodes have the same relay traffic input rates, the linear program solution in Eq. (40) approaches the maximum system throughput.

5.2. Transmission opportunity $p(x)$ design at hop level

In the preceding subsection we proposed a Poisson input traffic rate control strategy for a hybrid WMN. We can observe that higher transmission opportunity probabilities $p(x)$ should be assigned to the nodes with lower hop distances since they have to provide relay service for more packets form the nodes with higher hop distances. We proceed to develop a simple channel access probability set $p(x)$, $x = 1, \ldots, H$, design inspired by the result obtained in Eq. (40). Let us consider a network where the total service rate $N(H)p(H)/t_c$ at the H-hop nodes is equal to the total source input rate $N(H)\lambda_s(H)$ at the H-hop nodes, i.e.,

$$N(H)\frac{p(H)}{t_c} = N(H)\lambda_s(H). \tag{41}$$

The $(H-1)$-hop nodes have to provide a sufficient total service rate to relay the packets form the H-hop nodes and to send the source packets of the $(H-1)$-hop nodes. Noting that $N(H)p(H)/t_c$ is the highest possible relay packet input rate arriving at the $(H-1)$-hop nodes, we obtain

$$N(H-1)\frac{p(H-1)}{t_c} = N(H-1)\lambda_s(H-1) + N(H)\frac{p(H)}{t_c}. \tag{42}$$

With the same logic we obtain the channel access probability design strategy for all $p(x)$.

If we consider the case where all WMN nodes have the same local source input traffic rate λ_s, we can further simplify Eq. (42) to

$$N(H-1)\frac{p(H-1)}{t_c} = [N(H-1) + N(H)]\frac{p(H)}{t_c}, \tag{43}$$

and further obtain the design rule

$$p(x) = \frac{\sum_{i=x}^{H} N(i)}{N(x)}p(H), \quad x = 1, \ldots, H. \tag{44}$$

Form the above derivations, we observe that the total channel access probability of the x-hop nodes grows as x decreases, which matches the results obtained in [17,18].

We note that the special case (44) gives the same $p(x)$ values as Eq. (22) in [18]; however, our preceding derivation is more insightful and requires fewer computations.

For the forwarding probability set $q(x)$, $x = 1, \ldots, H$, our design strategy is to give fair transmission bitrate shares to traffic flows form nodes with different hop distances. For a uniform networking scenario where all nodes have the same source input rate, we can simply calculate the traffic amount in terms of node numbers, i.e.,

$$q(x) = \frac{\sum_{i=x+1}^{H} N(i)}{\sum_{i=x}^{H} N(i)}, \quad x = 1, \ldots, H, \tag{45}$$

where $\sum_{i=x+1}^{H} N(i)$ is the number of nodes with hop distance higher than x. Note that the resulting $q(x)$ corresponds to the portion of relay traffic to the total input traffic.

5.3. Network design at node level

In the previous subsection, we introduced the network design strategy at the hop distance level. In real practical network topologies, the hop-level design may degrade network performance since WMN nodes with the same hop distance may have different source input and relay traffic input rates. Service rates lower than the input traffic rates will lower throughout and increase delay. Hence, we propose the following channel access p_i and forwarding probability q_i design based on the traffic characteristics at individual nodes m_i. The individual node m_i level design follows the same overall strategy as the hop-count level design. That is, we equip each node m_i with the same service rate as its total input traffic rate. For WMN node m_i, the channel access probability design is

$$\frac{p_i}{t_c} = \sum_{j\in R_i}\frac{p_j}{f_j t_c} + \lambda_i, \tag{46}$$

where $\sum_{j\in R_i} p_j/(f_j t_c)$ is the highest relay traffic input rate. We note that for the edge nodes with hop distance H, $p_i = \lambda_i t_c$. For the forwarding probability, our design gives a fair share of the transmission bitrate to relay traffic:

$$q_i = \frac{\sum_{j\in R_i}\frac{p_j}{f_j t_c}}{\sum_{j\in R_i}\frac{p_j}{f_j t_c} + \lambda_i}. \tag{47}$$

In the next section, we will show that such a node level design can provide better performance than hop distance level designs.

6. Numerical evaluation

6.1. Evaluation set-up

6.1.1. Settings for numerical evaluations

For the numerical evaluations based on the throughput and delay analysis in Section 4, we set the time slot lengths for both the WMN and PON parts to the time needed to transmit one packet. The relay queues Q_r and local source queues Q_s are set to hold at most $K = 64$ packets. We report the specific parameter settings that varied for each of the evaluation scenarios in the captions of the result figures.

6.1.2. Simulation set-up

We based our discrete event simulation model on the OMNET++ simulation framework and implemented the specific WMN and PON packet forwarding functions through custom code modules. The buffer

size was set to $K = 64$ packets, whereby a standard Ethernet packet size of 1500 bytes was considered. Thus, the actual buffer size was 64·1500 bytes. Throughout, we report the throughput in units of packets per time slot. We note that the actual throughput in bytes/second is the throughput in packets per time slot multiplied by the ratio of packet size in byte to the time slot duration in seconds. We employed an independent Poisson packet generation process for each source queue.

We employed the batch means method to obtain statistical confidence intervals. We ran 25 batches with 400,000 packets recorded for each batch, plus a warm-up period with 400,000 packets, i.e., one warm-up batch that was not counted for the estimation of the performance metrics. Thus, 10,000,000 packets were recorded in total for a given simulation configuration. The resulting 98% confidence intervals for all simulation results are less than 2% of the corresponding sample means and are too small to be visible in the plots.

6.1.3. Network topology

Following the typical evaluation scenario from [17,18], we consider a network topology with 126 WMN nodes distributed on six concentric rings, as illustrated in Fig. 3. Ring h has a radius of $(55\,h)$ m and $6\,h$ WMN nodes are equally spaced on the ring. Each WMN node has a transmission range of $r = 100$ m. With these parameter settings: (a) Each WMN node can find at least one node within its transmission range on both adjacent inner and outer rings, but cannot find any node within its transmission range that is two or more rings away. (b) Each WMN node can communicate with its two neighbors on the same ring. This design ensures network robustness, even when it is divided into clusters. We form a FiWi network with Z clusters by partitioning the network topology evenly into Z circular sectors and positioning the gateways in the centroid of each circular sector. We note that for the special case of $Z = 1$ cluster, i.e., when the entire WMN forms one cluster that is served by a single ONU, the ONU gateway is positioned at the center of the network topology. For this special $Z = 1$ case, the positions of the wireless network nodes can be considered "uniform" with respect to the ONU in the center of the network topology. For larger numbers of clusters Z, $Z = 2, 3, \ldots 6$, as considered in our evaluation study, the wireless nodes have non-uniform positions with respect to the ONU (gateway) that is placed in the centroid of each of the corresponding Z circular sectors of the network topology. The optimized placement of ONUs is a separate research problem, see e.g., [60–63]; future research may examine optimized ONU placement in the context of our node level FiWi network design. Table 2 gives some basic FiWi network statistics with different numbers of clusters Z.

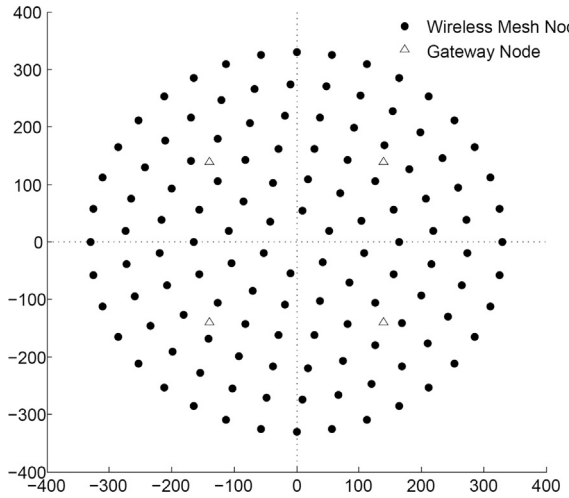

Fig. 3. Illustration of network topology with 126 WMN nodes positioned on rings h, $h = 1, 2, \ldots, 6$, with radius $(55\,h)$ m with $Z = 4$ clusters.

Table 2
FiWi network characteristics for different numbers of clusters Z: Average hop distance to ONU, maximum hop distance H in network, and number of nodes $N(1)$ with one hop to an ONU.

Z	Avg. dist	H	$N(1)$
1	4.333	6	6
2	2.714	5	20
3	2.143	4	33
4	1.810	3	42
5	1.667	3	52
6	1.667	3	54
7	1.540	3	64
8	1.508	3	68
9	1.500	3	69
10	1.476	3	72

6.2. Hop-distance level design

6.2.1. Controlled input traffic rate $\lambda(x)$ and channel access prob. $p(x)$ and forwarding prob. $q(x)$ settings

In this hop-distance level subsection, we consider scenarios where all x-hop nodes have the same channel access probability $p(x)$ and forwarding probability $q(x)$, i.e.,

$$p_i = p(x) \quad \forall \quad i \text{ such that } h_i = x \tag{48}$$

$$q_i = q(x) \quad \forall \quad i \text{ such that } h_i = x. \tag{49}$$

Each scenarios satisfies

$$\sum_{x=1}^{H} N(x)p(x) = 1, \tag{50}$$

which guarantees that at least one WMN node is granted the transmission opportunity per time slot. In particular, we control the bandwidth allocation according to two different settings for the channel access probability $p(x)$ and the forwarding probability $q(x)$:

pth: $p(x)$ is set according to Eq. (44) and $q(x)$ is set according to Eq. (45), see Table 3(a) and (b).
pde: $p(x)$ is set according to Eq. (44), see Table 3(a), and $q(x)$ is set to 0.975, which is higher than the value of Eq. (45).

We compare the controlled input traffic design with the network performance for heavy-loaded traffic. For the controlled traffic input rate, we assume that all x-hop nodes have the same source traffic rates, i.e.,

$$\lambda_i = \lambda(x) \quad \forall \quad i \text{ such that } h_i = x. \tag{51}$$

In particular, we set

$$\lambda(x) = \lambda_{s,\text{opt}}, \quad x = 1, \ldots, H, \tag{52}$$

where $\lambda_{s,\text{opt}}$ is obtained from Eq. (40) according to the channel access probability set. The actual values of $\lambda_{s,\text{opt}}$ used in the simulations are listed in Table 3(c).

In the heavy-loaded input traffic model, the source traffic queues Q_s are constantly backlogged [17,18,28,29]. In our simulations, we model the heavy-loaded traffic as Poisson input traffic with very high input rates. Specifically, we set

$$\lambda(x) = 5p(x), \quad x = 1, \ldots, H, \tag{53}$$

which ensures that the local source queues Q_s have a minimal traffic intensity equal to five. This ensures that the probability of a local queue Q_s being empty is approximately 5^{-64}.

The result figures employ the following labelling conventions. The "pth" and "pde" indicate the channel access and forwarding probability set. The "G" and "H" indicate controlled input traffic and heavy-loaded input traffic, respectively. Moreover, "sim" refers to results obtained via

Table 3
Channel access prob. $p(x)$ and forwarding prob. $q(x)$ as a function of hop distance x to gateway for pth setting as well as optimized controlled source input rate $\lambda_{s,\text{opt}}$ for different numbers of clusters Z.

(a) Channel access prob.$p(x)$ from Eq. (44)

Z	$p(1)$	$p(2)$	$p(3)$	$p(4)$	$p(5)$	$p(6)$
1	0.0385	0.0183	0.0110	0.0069	0.0040	0.0018
2	0.0184	0.0091	0.0053	0.0036	0.0029	n/a
3	0.0141	0.0068	0.0048	0.0037	n/a	n/a
4	0.0131	0.0056	0.0044	n/a	n/a	n/a
5	0.0115	0.0055	0.0047	n/a	n/a	n/a
6	0.0111	0.0057	0.0048	n/a	n/a	n/a
7	0.0101	0.0057	0.0051	n/a	n/a	n/a
8	0.0098	0.0059	0.0052	n/a	n/a	n/a
9	0.0097	0.0059	0.0052	n/a	n/a	n/a
10	0.0097	0.0058	0.0053	n/a	n/a	n/a

(b) Forwarding prob.$q(x)$ from Eq. (45)

Z	$q(1)$	$q(2)$	$q(3)$	$q(4)$	$q(5)$
1	0.9523	0.9	0.8333	0.7333	0.5454
2	0.8413	0.6792	0.4444	0.1875	n/a
3	0.7381	0.4516	0.2143	n/a	n/a
4	0.6667	0.2143	n/a	n/a	n/a
5	0.5873	0.1351	n/a	n/a	n/a
6	0.5714	0.1666	n/a	n/a	n/a
7	0.4920	0.0967	n/a	n/a	n/a
8	0.4603	0.1034	n/a	n/a	n/a
9	0.4524	0.1052	n/a	n/a	n/a
10	0.4285	0.1111	n/a	n/a	n/a

(c) $\lambda_{s,\text{opt}}$ from Eq. (40)

Z	pth and pde
1	0.0018
2	0.0029
3	0.0037
4	0.0043
5	0.0048
6	0.0048
7	0.0052
8	0.0053
9	0.0053
10	0.0054

simulation and "the" indicates results obtained via theoretical analysis presented in Section 4. To examine the effects of the channel access design on the overall FiWi network performance, we initially set the PON transmission bitrate to ten times the total WMN transmission bitrate.

6.2.2. Results: Impact of controlled input traffic

Fig. 4 shows the mean throughput and delay of the pth and pde settings for controlled and heavy-loaded input traffic. We note that the heavy-loaded traffic attains the maximum system throughput since the (essentially) constantly backlogged local source traffic queues ensure that every channel access opportunity is utilized [18,17]. With heavy-loaded traffic, the utilization levels of the channel access opportunities (transmission resources) provided by the underlying network are high, i.e., the traffic intensities are high. We observe from Fig. 4 that for both the pth and pde settings, the proposed controlled input traffic design (Section 5.1) achieves about 80% of the maximum system throughput (which is achieved with heavy-loaded traffic), while reducing the delay to half or less compared to the heavy-loaded traffic.

The throughput reduction is due to some missed transmission opportunities, i.e., transmission opportunities that are assigned to a node but cannot be utilized since there is no relay traffic and no source input traffic available for transmission. That is, with the input traffic control, the utilization level of the network transmission resources is lower than with the heavy-loaded traffic. The delay comparison in Fig. 4 indicates that the input traffic control approximately halves the mean packet delay compared to heavy-loaded traffic. This delay reduction is due to the somewhat lower traffic loads that result from the control of the input traffic such that each hop distance level can better (i.e., in a more timely manner) accommodate the relay traffic load arriving from the preceding hop level, see Eq. (39). In other words, the lower utilization levels of the network transmission resources, i.e., the lower traffic intensities, with the input traffic control result in lower mean packet delays than with the heavy-loaded traffic.

6.2.3. Results: Impact of forwarding probabilities $q(x)$

Prior heavy-load studies, e.g., [18,17], found that compared to the pth setting, the pde setting can lower mean delays while achieving the same system throughput. Note that heavy traffic studies, such as [18,17], typically considered only the queueing delays in the relay queues (and not the queueing delay in the source nodes). We consider the queueing delays in both source and relay nodes throughout this study for both our controlled [G, see Eq. (52)] and heavy [H, see Eq. (53)] Poisson traffic. We observe from Fig. 4 that for the controlled traffic load, the pth and pde settings result in essentially equivalent mean delays. This observation can be explained as follows. The

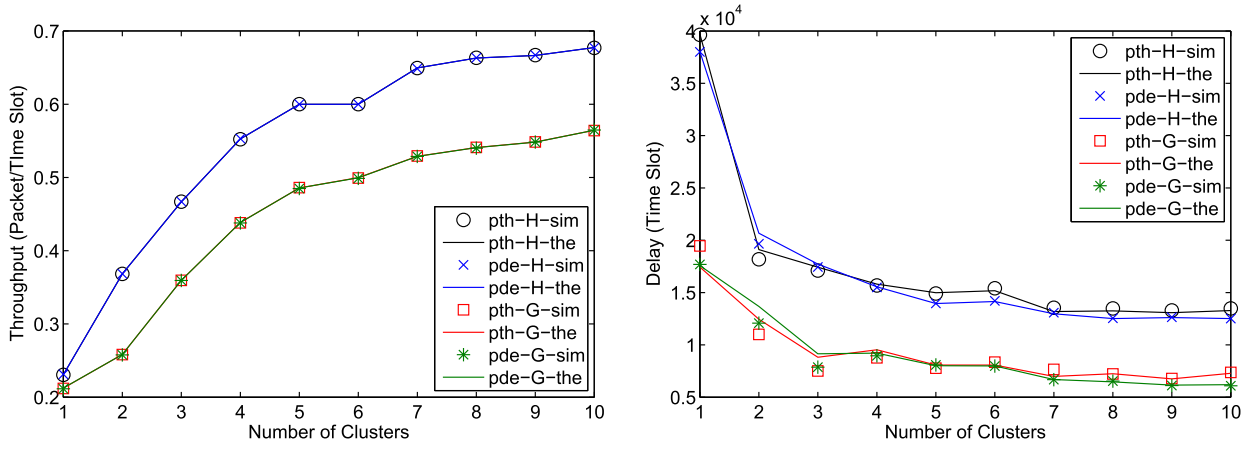

(a) Throughput (b) Delay

Fig. 4. Mean FiWi network throughput and delay with hop distance level design (Sections 5.1 and 5.2) as a function of number of clusters Z for pth and pde settings with controlled (G) and heavy (H) loaded traffic. (For pth and pde settings, nodes with the same hop distance x have the same channel access probability $p(x)$ and forwarding probability $q(x)$ according to Eqs. (48)–(50). Specifically, for the pth setting, $p(x)$ is obtained from Eq. (44) and listed in Table 3(a), $q(x)$ is obtained from Eq. (45) and listed in Table 3(b). For the pde setting, $p(x)$ is obtained from Eq. (44) and listed in Table 3(a), $q(x) = 0.975$ fixed. For controlled traffic (G), all nodes (in both pth and pde) have the same source packet traffic input rate $\lambda_i = \lambda_{s,\text{opt}}$ obtained via Eq. (40) and listed in Table 3(c). For heavy-loaded traffic (H), $\lambda(x) = 5p(x)$).

transmission opportunities at a WMN node are shared by its source and relay queues. Thus, allocating a transmission opportunity to one queue introduces delay to the other queue. The pde setting strongly prioritizes the relay queue. However, this relay queue prioritization delays service to the source queue. If only relay queue delays are considered, then the pde setting does result in delay reductions, as reported in heavy traffic studies, such as [18,17]. On the other hand, when considering the queueing delays in the source as well as the relay queues, the pde setting does not reduce the mean delay since the delay reductions of the relay traffic are achieved at the expense of increasing the source queue delays.

We note that the heavy traffic model has often been adopted in analytical studies for ease of tractability. However, in practical networks, traffic is usually non-heavy and the delays in the source nodes do matter for the end-to-end delays experienced by applications. We caution therefore that the previously reported results obtained for heavy traffic may be misleading by indicating delay reductions for the pde setting compared to the pth setting. As demonstrated by our results in Fig. 4, the pde setting does in fact *not* reduce the practically relevant end-to-end mean delays for non-heavy traffic models. We also note that for practically relevant non-heavy traffic, there are some differences between the pde and pth settings, in that pde improves the performance specifically for the nodes with higher hop distances, as examined in Section 6.3.3.

6.3. Node level design

6.3.1. Channel access probability $p(x)$ and forwarding probability $q(x)$ settings

In this subsection, we study the system performance for the channel access probability $p(x)$ design at the level of individual nodes (see Section 5.3), which allows each WMN node m_i to have a different channel access probability p_i and forwarding probability q_i. Analogously to the hop distance design, we set

$$\sum_{i=1}^{N} p_i = 1. \tag{54}$$

The values of p_i and q_i are designed according to Eqs. (46) and (47). For $\lambda_{s,i} = \lambda_s$, we find that with

$$\lambda_s = \frac{1}{\sum_{i=1}^{N} h_i}, \tag{55}$$

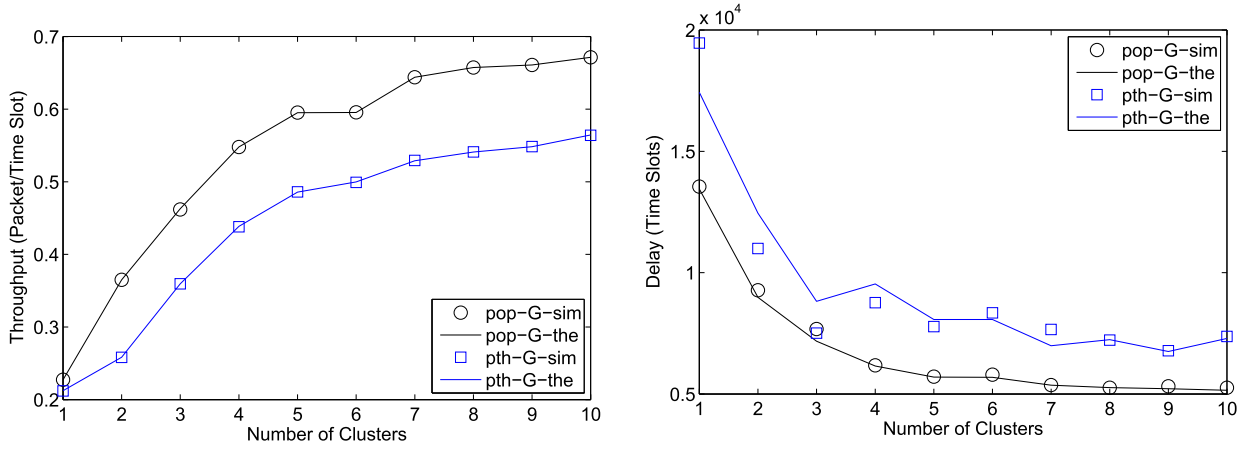

(a) Throughput (b) Delay

Fig. 5. FiWi network performance comparison of node level design (pop) and hop distance level design (pth). (For pop settings, each node can have different channel access probability p_i obtained via Eq. (46) and forwarding probability q_i obtained via Eq. (47). For controlled pop traffic (G), all nodes have the same source packet input rate $\lambda_{s,i} = \lambda_s$ with λ_s given by Eq. (55)).

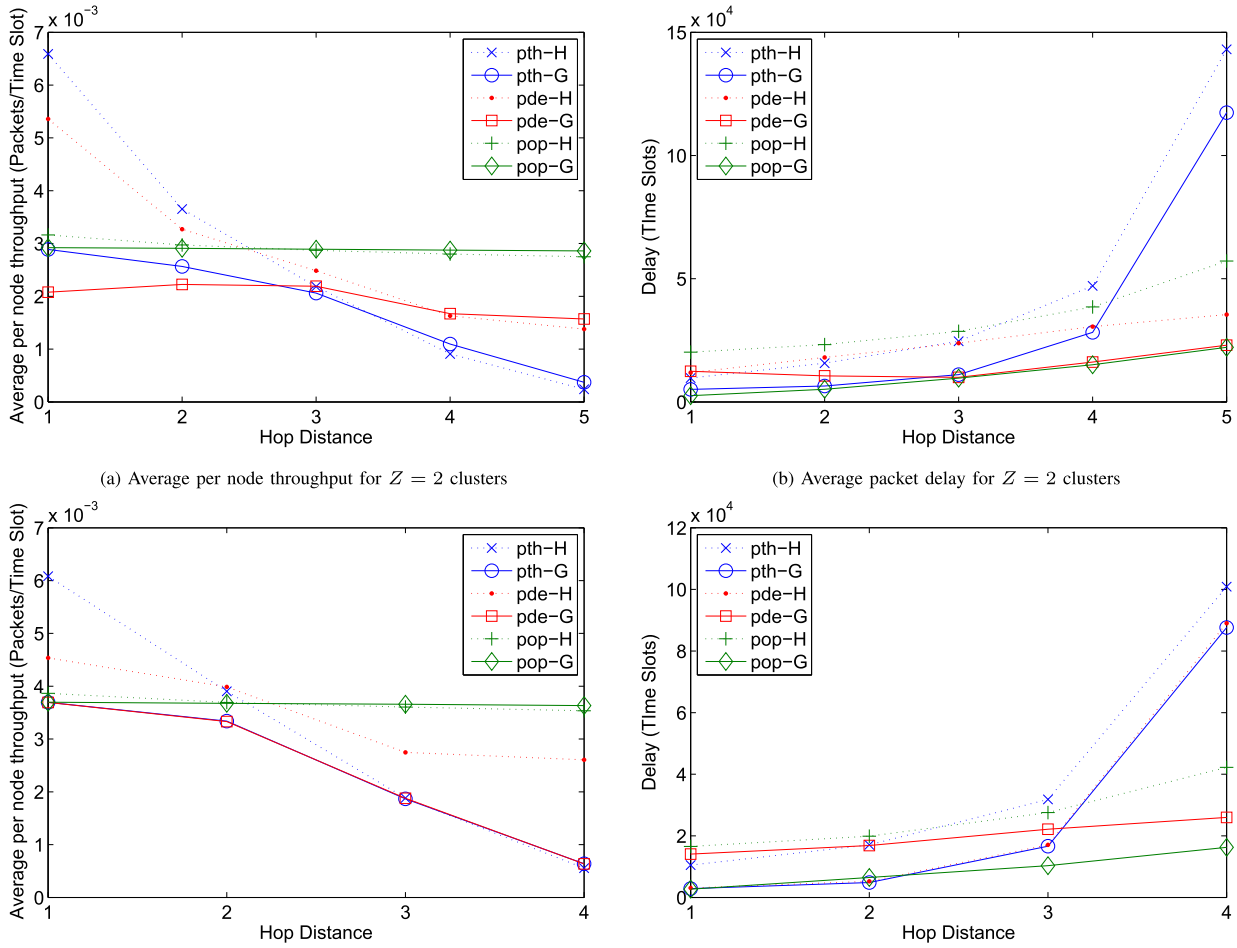

(a) Average per node throughput for $Z = 2$ clusters

(b) Average packet delay for $Z = 2$ clusters

(c) Average per node throughput for $Z = 3$ clusters

(d) Average packet delay for $Z = 3$ clusters

Fig. 6. Mean per node throughput and delay as a function of hop distance from the gateway (ONU). (The pth and pde scenarios follow the parameter settings summarized in the caption of Fig. 4, while pop-G follows the parameter settings as per the caption of Fig. 5. The pop-H scenario has source input traffic rate $\lambda_{s,i} = 5p_i$).

Eq. (54) is satisfied. We refer to this per-node level transmission/forwarding probability design as "pop".

6.3.2. Results: Node level design vs. hop level design

Fig. 5 compares the pop node level design with the pth hop distance level design for controlled input traffic. We observe from Fig. 5 that pop achieves higher throughput and lower delay than pth. (We found in additional evaluations that are not included here to avoid clutter that pth with heavy traffic achieves the same throughput as pop with controlled input traffic.) The higher throughput and lower delay with the pop design are due to the individualized per-node assignments of the channel access probability p_i and forwarding probability q_i according to the traffic characteristics at each individual node m_i. This per-node assignment is computationally still very simple, see Eqs. (46) and (47), and relies on the sets R_i of preceding hop nodes, which are readily available for static WMNs.

6.3.3. Results: Nodes with different hop distances

In this subsection, we study the throughput and delay performance experienced by nodes that have different hop distances from the ONU. Fig. 6 shows the average per-node throughput and delay experienced by nodes that require between one and four hops to reach in ONU in FiWi networks with $Z = 2$ and 3 clusters. We observe from Fig. 6 that pth has the most pronounced performance imbalance in that nodes with short hop distances experience much higher per-node throughput and shorter average delays than nodes with higher hop distances; and this imbalance worsens for the heavy-loaded input traffic. The pde setting balances the performance somewhat better compared to pth; however, nodes with lower hop distances still tend to experience both better throughput and delay performance. We further observe from Fig. 6 that the pop setting provides consistently fair per-node throughput to nodes at all hop distances and has the mildest delay imbalance. This fair pop performance with respect to the different hop distances to the ONU is achieved through the individualized per-node channel access and forwarding probabilities based on the traffic characteristics at each individual node m_i. We acknowledge that the nodes with higher hop distances to the ONU tend to have higher delays, even with the pop design, and this higher delay for higher hop distances is the general nature of multi-hop networks that would be very difficult to completely eliminate [64,18]. Overall, we conclude that for balanced FiWi system performance, the pop node level channel access probability and forwarding probability design (see Section 5.3) achieves relatively consistent and fair throughput-delay performance for the nodes at the various hop distances from the ONUs.

6.4. Impact of PON DBA

Generally, in FiWi networks, the effects of the PON part become most noticeable when the WMN output rate approaches or even exceeds the PON service rate [38,17,62,36]. In this subsection, we examine the effects of the PON DBA in the context of the pth setting with controlled input traffic. We set the PON service rate to half of the WMN rate, i.e., 0.5 (packet/time slot) is the maximum FiWi throughput. Fig. 7 shows the PON delay and throughput as a function of the

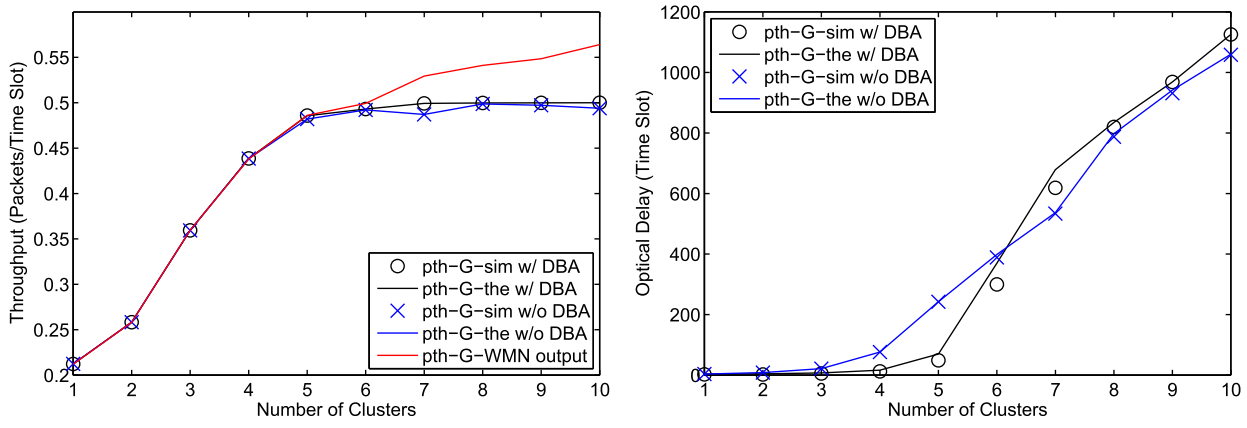

(a) Throughput (b) Delay

Fig. 7. Mean PON throughput and delay as a function of number of clusters Z for pth setting and controlled traffic. (The pth-G scenario follows the parameter settings summarized in the caption of Fig. 4).

number of clusters Z. We observe from Fig. 7 that for scenarios when the WMN output rates are relative lower than the PON service rate (0.5 packets/time slot), the PON introduces negligible delay and the effect of the DBA is not significant. For $Z = 4$ to 6, where the WMN output rates are close to the PON service rate, we observe that the DBA is capable of reducing the optical delay by assigning the bandwidth according to the input traffic of each ONU. For $Z \geq 7$, we observe that the DBA introduces very slight PON delay increases while achieving very slightly higher throughput compared to the fixed PON bandwidth allocation without DBA. This is due to the fact that for the non-DBA scheme, some ONUs have traffic intensity larger than one, while other ONUs have intensity lower than one. Such imbalanced situations result in slightly reduced throughput and slightly lower delay due to ONUs that do not fully use their fixed bandwidth allocation. Overall, we conclude that a DBA helps to compensate for load imbalances among the ONUs. The results also show that our approximate $M/M/1/K$ queue modeling approach (see Section 4.7.2) achieves a reasonably close characterization of the DBA performance.

7. Conclusion

We have analyzed the throughput-delay characteristics of Fiber-Wireless (FiWi) networks formed by connecting clusters of Wireless Mesh Network (WMN) nodes via a Passive Optical Network (PON) to a central Optical Line Terminal (OLT). Each WMN node cluster is served by a dedicated Optical Network Unit (ONU) of the PON. In contrast to existing analyses that have considered heavy-loaded WMN nodes that are constantly backlogged, we have developed general delay-throughput models that accommodate non-heavy Poisson traffic as well as the effects of dynamic bandwidth allocation (DBA) in the PON. Based on the formalisms and insights gained from our throughput-delay analysis, we have developed (*i*) a novel traffic control strategy that limits the source traffic injected at the WMN nodes into the FiWi network, and (*ii*) novel node-level assignments of channel access probabilities for WMN nodes and forwarding probabilities for relay packets at the WMN nodes.

Our extensive numerical evaluations have verified the accuracy of the developed analytical throughput-delay models. We found that prior studies with heavy traffic reported the misleading result that high forwarding probability settings would reduce the mean packet delay. However, these prior studies considered only the delay in the relay queues and not in the source queue of the node that generated the packet. Our more general non-heavy traffic model accommodates the source queue delay and demonstrates that prior reported high forwarding probability settings do in fact *not* reduce the mean packet delay. However, the proposed traffic control and the proposed node-level channel access and forwarding probability design do reduce the mean packet delays. Also, the evaluations indicate that the proposed node level channel access and forwarding probability design can achieve balanced throughput-delay performance at WMN nodes with different hop distances to the ONUs.

There are several important directions for future research on FiWi network analysis. One direction is to examine mechanisms for achieving low delays for interactive applications, such as augmented reality applications [65–67]. Such low-delay interactive applications could be further supported through the integration of edge computing into the FiWi network [68–71] and advanced control paradigms, such as software defined networking control [72,73]. Another direction is to examine the integrated control and network management of FiWi networks across multiple OLTs and metropolitan areas [74–78]. Such integrated control and management mechanisms could judiciously interface the FiWi MAC and scheduling mechanisms with metropolitan area network MAC protocols [79–83]. Yet another future research direction is to expand the performance evaluation to consider energy saving mechanisms, such as integrated sleep modes [84,85].

Appendix A. Summary of $M/M/1/K$ and $M/D/1/K$ queues

For packet arrival rate λ and packet service rate μ, the traffic intensity is $\rho = \lambda/\mu$. Consider an $M/M/1/K$ queue that can hold up to K packets. The queue holds K packets, i.e., blocks newly arriving packets, with probability [55]:

$$P_{M,K}(\rho, K) = \begin{cases} \dfrac{(1-\rho)\rho^K}{1-\rho^{K+1}} & \text{if } \rho \neq 1 \\ \dfrac{1}{K+1} & \text{if } \rho = 1. \end{cases} \tag{56}$$

The queue is empty with probability

$$P_{M,0}(\rho, K) = \begin{cases} \dfrac{1-\rho}{1-\rho^{K+1}} & \text{if } \rho \neq 1 \\ \dfrac{1}{K+1} & \text{if } \rho = 1. \end{cases} \tag{57}$$

The average queue length is [55]:

$$L_M(\rho, K) = \begin{cases} \dfrac{\rho}{1-\rho} - \dfrac{\rho(K\rho^K+1)}{1-\rho^{K+1}} & \text{if} \rho \neq 1 \\ \dfrac{K(K-1)}{2(K+1)} & \text{if } \rho = 1 \end{cases} \tag{58}$$

and the average waiting time is

$$W_M(\mu, \lambda, K) = \frac{1}{\mu} + \frac{L_M(\rho, K)}{\lambda[1 - P_{M,K}(\rho, K)]}. \tag{59}$$

Denote $P_{D,k}(\rho, K)$, $k = 0, \ldots, K$, for the stationary state probabilities of holding k packets in an $M/D/1/K$ queue. For $0 \leq k \leq K-1$, the recursion [55]

$$P_{D,k}(\rho, K) = \lambda a_{k-1} P_{D,0}(\rho, K) + \lambda \sum_{j=1}^{k} a_{k-j} P_{D,j}(\rho, K), \tag{60}$$

with $a_n = \frac{1}{\lambda}(1 - \sum_{j=1}^{n} e^{-\rho}\rho^j/j!)$, start at $P_{D,0} = 1$, and normalization with $\sum_{i=0}^{K} P_{D,i}(\rho, K) = 1$ gives the steady state probabilities. The blocking probability, i.e., the Kth state probability, is

$$P_{D,K}(\rho, K) = \rho P_{D,0}(\rho, K) - (1-\rho) \sum_{j=1}^{K-1} P_{D,j}(\rho, K). \tag{61}$$

Alternatively, [86] gives an explicit formula for $P_{D,k}(\rho, K)$, which can become computationally demanding for large K [87]. The average waiting time of an $M/D/1/K$ queue follows with Little's Law as

$$W_D(\mu, \lambda, K) = \frac{1}{\mu} + \frac{L_D(\rho, K)}{\lambda[1 - P_{D,K}(\rho, K)]}, \tag{62}$$

where $L_D(\rho, K) = \sum_{k=0}^{K} k P_{D,k}(\rho, K)$ is the average $M/D/1/K$ queue length.

References

[1] M.G. Bade, M. Toycan, S.D. Walker, Cost and energy efficient operation of converged, reconfigurable optical wireless networks, Opt. Switch. Netw. 18 (Part 1) (2015) 71–80.
[2] J. Coimbra, G. Schtz, N. Correia, A game-based algorithm for fair bandwidth allocation in Fibre-Wireless access networks, Opt. Switch. Netw. 10 (2) (2013) 149–162.
[3] J. Liu, H. Guo, H. Nishiyama, H. Ujikawa, K. Suzuki, N. Kato, New perspectives on future smart FiWi networks: scalability, reliability, and energy efficiency, IEEE Commun. Surv. Tutor. 18 (2) (2016) 1045–1072.
[4] Y. Liu, J. Wu, Y. Yu, Z. Ning, X. Wang, K. Zhao, Deployment of survivable fiber-wireless access for converged optical and data center networks, Opt. Switch. Netw. 14 (Part 3) (2014) 226–232.
[5] R. Upadhyay, U.R. Bhatt, N. Chouhan, T. Sarsodia, Computation of various QoS parameters for FiWi access network, Procedia Comput. Sci. 78 (2016) 172–178.
[6] N. Zaker, B. Kantarci, M. Erol-Kantarci, H.T. Mouftah, Smart grid monitoring with service differentiation via EPON and wireless sensor network convergence, Opt. Switch. Netw. 14 (August (Part 1)) (2014) 53–68.
[7] P. Bhaumik, A.S. Reaz, D. Murayama, K.-I. Suzuki, N. Yoshimoto, G. Kramer, B. Mukherjee, IPTV over EPON: synthetic traffic generation and performance evaluation, Opt. Switch. Netw. 18 (Part 2) (2015) 180–190.
[8] A. Buttaboni, M.D. Andrade, M. Tornatore, A. Pattavina, Dynamic bandwidth and wavelength allocation with coexisting transceiver technology in WDM/TDM PONs, Opt. Switch. Netw. 21 (2016) 31–42.
[9] M.D. Andrade, A. Buttaboni, M. Tornatore, P. Boffi, P. Martelli, A. Pattavina, Optimization of long-reach TDM/WDM passive optical networks, Opt. Switch. Netw. 16 (2015) 36–45.
[10] S.M.F.S.F. Gillani, M.A. Khan, M.K. Shahid, Reach extendibility of passive optical network technologies, Opt. Switch. Netw. 18 (Part 3) (2015) 211–221.
[11] X. Gong, L. Guo, Y. Liu, Y. Zhou, H. Li, Optimization mechanisms in multi-dimensional and flexible PONs: challenging issues and possible solutions, Opt. Switch. Netw. 18 (Part 1) (2015) 120–134.
[12] A. Kanungoe, A. Mukhopadhyay, G. Das, R. Banerjee, R. Das, A new protection scheme for a combined ring-star based hybrid WDM/TDM PON architecture, Opt. Switch. Netw. 18 (Part 2) (2015) 153–168.
[13] J.-R. Lai, W.-P. Chen, High utilization dynamic bandwidth allocation algorithm based on sorting report messages with additive-polling thresholds in EPONs, Opt. Switch. Netw. 18 (Part 1) (2015) 81–95.
[14] M. Mahloo, J. Chen, L. Wosinska, PON versus AON: which is the best solution to offload core network by peer-to-peer traffic localization, Opt. Switch. Netw. 15 (2015) 1–9.
[15] M.P. McGarry, M. Reisslein, F. Aurzada, M. Scheutzow, Shortest propagation delay (SPD) first scheduling for EPONs with heterogeneous propagation delays, IEEE J. Sel. Areas Commun. 28 (6) (2010) 849–862.
[16] A. Mercian, M.P. McGarry, M. Reisslein, Offline and online multi-thread polling in long-reach PONs: a critical evaluation, IEEE/OSA J. Lightw. Technol. 31 (12) (2013) 2018–2028.
[17] P.-Y. Chen, M. Reisslein, A simple analytical throughput-delay model for clustered FiWi networks, Photon. Netw. Commun. 29 (February (1)) (2015) 78–95.
[18] T. Liu, W. Liao, Location-dependent throughput and delay in wireless mesh networks, IEEE Trans. Veh. Technol. 57 (March (2)) (2008) 1188–1198.
[19] P. Li, C. Zhang, Y. Fang, Capacity and delay of hybrid wireless broadband access networks, IEEE J. Sel. Areas Commun. 27 (February (2)) (2009) 117–125.
[20] D. Shila, Y. Cheng, T. Anjali, Throughput and delay analysis of hybrid wireless networks with multi-hop uplinks, Proc. IEEE Info. (2011) 1476–1484.
[21] D. Wang, A.A. Abouzeid, Throughput and delay analysis for hybrid radio-frequency and free-space-optical (RF/FSO) networks, Wirel. Netw. 17 (4) (2011) 877–892.
[22] A. Zemlianov, G. de Veciana, Capacity of ad hoc wireless networks with infra-structure support, IEEE J. Sel. Areas Commun. 23 (March (3)) (2005) 657–667.
[23] Y. Feng, X. Shen, Z. Gao, G. Dai, Queuing based traffic model for wireless mesh networks, Proc. IEEE ICPADS (2009) 648–654.
[24] W. Liu, D. Zhao, G. Zhu, End-to-end delay and packet drop rate performance for a wireless sensor network with a cluster-tree topology, Wirel. Commun. Mob. Comp. 14 (May (7)) (2014) 729–744.
[25] V.S. Naeini, Performance analysis of WiMAX-based wireless mesh networks using an M/D/1 queuing model, Int. J. Wirel. Mob. Comp. 7 (1) (2014) 35–47.
[26] Y. Chen, J. Chen, Y. Yang, Multi-hop delay performance in wireless mesh networks, Mob. Netw. Appl. 13 (1–2) (2008) 160–168.
[27] S. Pandey, V. Tambakad, G. Kadambi, Y. Vershinin, An analytic model for route optimization in load shared wireless mesh network, Proc. IEEE EMS (2013) 543–548.
[28] W. Tu, C. Sreenan, Adaptive split transmission for video streams in wireless mesh networks, Proc. IEEE WCNC (2008) 3122–3127.
[29] F.R. Vieira, J.F. de Rezende, V.C. Barbosa, S. Fdida, Scheduling links for heavy traffic on interfering routes in wireless mesh networks, Comput. Netw. 56 (5) (2012) 1584–1598.

[30] N. Bisnik, A. Abouzeid, Queuing network models for delay analysis of multihop wireless ad hoc networks, Ad Hoc Netw. 7 (1) (2009) 79–97.
[31] F. Wang, O. Younis, M. Krunz, Throughput-oriented MAC for mobile ad hoc networks: a game-theoretic approach, Ad Hoc Netw. 7 (1) (2009) 98–117.
[32] Y. Dashti, M. Reisslein, CluLoR: clustered localized routing for FiWi networks, J. Netw. 9 (4) (2014) 828–839.
[33] S. He, G. Shou, Y. Hu, Z. Guo, Performance of multipath in Fiber-Wireless (FiWi) access network with network virtualization, Proc. IEEE Milcom (2013) 928–932.
[34] M. Honda, H. Nishiyama, H. Nomura, T. Yada, H. Yamada, N. Kato, On the performance of downstream traffic distribution scheme in fiber-wireless networks, Proc. IEEE WCNC (2011) 434–439.
[35] S. Li, J. Wang, C. Qiao, Y. Xu, Mitigating packet reordering in FiWi networks, IEEE/OSA J. Opt. Commun. Netw. 3 (February (2)) (2011) 134–144.
[36] J. Wang, K. Wu, S. Li, C. Qiao, Performance modeling and analysis of multi-path routing in integrated fiber-wireless networks, Proc. IEEE Info. (2010) 1–5.
[37] Z. Zheng, J. Wang, J. Wang, A study of network throughput gain in optical-wireless (FiWi) networks subject to peer-to-peer communications, Proc. IEEE ICC (2009) 1–6.
[38] F. Aurzada, M. Levesque, M. Maier, M. Reisslein, FiWi access networks based on next-generation PON and gigabit-class WLAN technologies: a capacity and delay analysis, IEEE/ACM Trans. Netw. 22 (August (4)) (2014) 1176–1189.
[39] A. Dhaini, P.-H. Ho, X. Jiang, QoS control for guaranteed service bundles over Fiber-Wireless (FiWi) broadband access networks, IEEE/OSA J. Lightw. Technol. 29 (May (10)) (2011) 1500–1513.
[40] A.R. Dhaini, P.-H. Ho, X. Jiang, Performance analysis of QoS-aware layer-2 VPNs over fiber-wireless (FiWi) networks, Proc. IEEE Globecom (2010) 1–6.
[41] M. Fadlullah, H. Nishiyama, Y. Kawamoto, H. Ujikawa, K.-I. Suzuki, N. Yoshimoto, Cooperative QoS control scheme based on scheduling information in FiWi access network, IEEE Trans. Emerg. Top. Comput. 1 (December (2)) (2013) 375–383.
[42] Y. Lee, S. Choi, Y. Choi, End-to-end delay differentiation mechanism for integrated EPON-WiMAX networks, Photon. Netw. Commun. 27 (2) (2014) 73–79.
[43] B.P. Rimal, M. Maier, Mobile data offloading in FiWi enhanced LTE-A heterogeneous networks, IEEE/OSA J. Opt. Commun. Netw. 9 (7) (2017) 601–615.
[44] J. Wang, K. Lu, J. Wang, C. Qiao, A joint network coding and device association design for optimal local data exchange in fiber-wireless access network, IEEE/OSA J. Lightw. Technol. 35 (11) (2017) 2046–2062.
[45] A. Barradas, N. Correia, J. Coimbra, G. Schutz, Load adaptive and fault tolerant framework for energy saving in fiber-wireless access networks, IEEE/OSA J. Opt. Commun. Netw. 5 (September (9)) (2013) 957–967.
[46] R.A. Butt, S.M. Idrus, K.N. Qureshi, P.M.A. Shah, N. Zulkifli, An energy efficient cyclic sleep control framework for ITU PONs, Opt. Switch. Netw. 27 (2018) 7–17.
[47] B. Kantarci, H. Mouftah, Energy efficiency in the extended- r each fiber-wireless access networks, IEEE Netw. 26 (March (2)) (2012) 28–35.
[48] G.C. Sankaran, K.M. Sivalingam, ONU buffer reduction for power efficiency in passive optical networks, Opt. Switch. Netw. 10 (4) (2013) 416–429.
[49] K. Togashi, H. Nishiyama, N. Kato, H. Ujikawa, K.-I. Suzuki, N. Yoshimoto, Cross layer analysis on ONU energy consumption in smart FiWi networks, IEEE Wirel. Commun. Lett. 2 (December (6)) (2013) 695–698.
[50] R. Wang, A. Liang, D. Wu, D. Wu, Delay-aware adaptive sleep mechanism for green wireless-optical broadband access networks, Opt. Fiber Technol. 36 (2017) 271–280.
[51] R. Wang, A. Liang, C. Zhou, D. Wu, H. Zhang, QoS -aware energy-saving mechanism for hybrid optical-wireless broadband access networks, Photon. Netw. Commun. 34 (2) (2017) 170–180.
[52] I.F. Akyildiz, X. Wang, W. Wang, Wireless mesh networks: a survey, Comp. Netw. 47 (4) (2005) 445–487.
[53] R. Bruno, M. Conti, E. Gregori, Mesh networks: commodity multihop ad hoc networks, IEEE Commun. Mag. 43 (3) (2005) 123–131.
[54] G. Bianchi, Performance analysis of the IEEE 802.11 distributed coordination function, IEEE J. Sel. Areas Commun. 18 (3) (2000) 535–547.
[55] D. Gross, C.M. Harris, Fundamentals of Queuing Theory, Wiley-Interscience, 1998.
[56] A. Bontozoglou, K. Yang, K. Guild, A midterm DBA algorithm for quality of service on aggregation layer EPON networks, Photon. Netw. Commun. 25 (2) (2013) 120–134.
[57] M.P. McGarry, M. Reisslein, Investigation of the DBA algorithm design space for EPONs, J. Lightw. Technol. 30 (14) (2012) 2271–2280.
[58] C.-C. Sue, K.-C. Chuang, Y.-T. Wu, S.-J. Lin, C.-C. Liu, Active intra-ONU scheduling with proportional guaranteed bandwidth in long-reach EPONs, Photon. Netw. Commun. 27 (3) (2014) 106–118.
[59] L. Zhou, H.-L. Wong, Y.-K. Yeo, X. Cheng, X. Shao, Z. Xu, Traffic scheduling in hybrid WDM-TDM PON with wavelength-reuse ONUs, Photon. Netw. Commun. 24 (2) (2012) 151–159.
[60] U.R. Bhatt, N. Chouhan, R. Upadhyay, Hybrid algorithm: a cost efficient solution for ONU placement in Fiber-Wireless (FiWi) network, Opt. Fiber Technol. 22 (2015) 76–83.
[61] U.R. Bhatt, N. Chouhan, R. Upadhyay, C. Agrawal, ONU placement in fiber-wireless (FiWi) access networks using teacher phase of Teaching Learning Based Optimization (TLBO) algorithm, in: Proceedings IEEE International Conference on Computational Intelligence & Commun. Techn. (CICT), 2017, pp. 1–4.
[62] Y. Liu, Q. Song, B. Li, R. Ma, Load balanced optical network unit (ONU) placement in cost-efficient fiber-wireless (FiWi) access network, Opt.-Int. J. Light Electron Opt. 124 (20) (2013) 4594–4601.
[63] P. Singh, S. Prakash, Optical network unit placement in fiber-wireless (FiWi) access network by Moth-Flame optimization algorithm, Opt. Fiber Technol. 36 (2017) 403–411.
[64] V. Gambiroza, B. Sadeghi, E.W. Knightly, End-to-end performance and fairness in multihop wireless backhaul networks, in: Proceedings ACM MobiCom, 2004, pp. 287–301.
[65] T. Jiménez, N. Merayo, R.J. Durán, P. Fernández, I. De Miguel, J.C. Aguado, R.M. Lorenzo, E.J. J. Abril, A PID-based algorithm to guarantee QoS delay requirements in LR-PONs, Opt. Switch. Netw. 14 (2014) 78–92.
[66] K. Kunert, M. Jonsson, A. Böhm, T. Nordström, Providing efficient support for real-time guarantees in a fibre-optic AWG-based network for embedded systems, Opt. Switch. Netw. 24 (2017) 47–56.
[67] A. Pašić, P. Babarczi, A. Kőrösi, Diversity coding-based survivable routing with QoS and differential delay bounds, Opt. Switch. Netw. 23 (2017) 118–128.
[68] X. Gong, L. Guo, G. Shen, G. Tian, Virtual network embedding for collaborative edge computing in optical-wireless networks, IEE/OSA J. Lightw. Technol. 35 (18) (2017) 3980–3990.
[69] B.P. Rimal, D.P. Van, M. Maier, Cloudlet enhanced fiber-wireless access networks for mobile-edge computing, IEEE Trans. Wirel. Commun. 16 (6) (2017) 3601–3618.
[70] B.P. Rimal, D.P. Van, M. Maier, Mobile edge computing empowered fiber-wireless access networks in the 5G era, IEEE Commun. Mag. 55 (2) (2017) 192–200.
[71] B.P. Rimal, D.P. Van, M. Maier, Mobile-edge computing vs. centralized cloud computing over a converged fiwi access network, IEEE Trans. Netw. Serv. Manag. 14 (3) (2017) 498–513.
[72] N. Cvijetic, T. Wang, Systems challenges for SDN in fiber wireless networks, in Fiber-Wireless Convergence in Next-Generation Communication Networks. Cham, Switzerland: Springer, 2017, pp. 189–209.
[73] A.S. Thyagaturu, A. Mercian, M.P. McGarry, M. Reisslein, W. Kellerer, Software defined optical networks (SDONs): a comprehensive survey, IEEE Commun. Surv. Tutor. 18 (4) (2016) 2738–2786.
[74] R. Brenot, G. De Valicourt, Telecommunications network node linking a metropolitan area network with at least one access network, Jan. 3 2017, US Patent 9, 537,597.
[75] X. Cao, I. Popescu, G. Chen, H. Guo, N. Yoshikane, T. Tsuritani, J. Wu, I. Morita, Optimal and dynamic virtual datacenter provisioning over metro-embedded datacenters with holistic SDN orchestration, Opt. Switch. Netw. 24 (2017) 1–11.
[76] Y. Hou, H. Li, Y. Liu, Y. Qiu, Y. Ji, OpenFlow-based adaptive adjustment of optical path resources in dynamic optical networks, Opt. Switch. Netw. 22 (2016) 105–116.
[77] W. Xia, C. Gan, S. Ma, L. Xu, W. Xie, Multi-channel scheduling algorithm for multi-subsystem-based VPON in metro-access optical network, Opt. Switch. Netw. 21 (2016) 58–66.
[78] Y. Zhang, C. Gan, K. Gou, J. Hua, GPON-and-EPON transmission based on multi-standard OLT management structure for VPON in metro-access optical network, Opt. Switch. Netw. 25 (2017) 24–32.
[79] A. Bianco, T. Bonald, D. Cuda, R.-M. Indre, Cost, power consumption and performance evaluation of metro networks, IEEE/OSA J. Opt. Commun. Netw. 5 (1) (2013) 81–91.
[80] M. Maier, M. Reisslein, A. Wolisz, A hybrid MAC protocol for a metro WDM network using multiple free spectral ranges of an arrayed-waveguide grating, Comput. Netw. 41 (4) (2003) 407–433.
[81] M. Scheutzow, M. Maier, M. Reisslein, A. Wolisz, Wavelength reuse for efficient packet-switched transport in an AWG-based metro WDM network, IEEE J. Lightw. Technol. 21 (6) (2003) 1435–1455.
[82] H.-S. Yang, M. Maier, M. Reisslein, W.M. Carlyle, A genetic algorithm-based methodology for optimizing multiservice convergence in a metro WDM network, IEEE/OSA J. Lightw. Technol. 21 (5) (2003) 1114–1133.
[83] A.X. Zheng, L. Zhang, V.W. Chan, Metropolitan area network architecture for optical flow switching, IEEE/OSA J. Opt. Commun. Netw. 9 (6) (2017) 511–523.
[84] M. Bokhari, M. Sohail, J.K. Kasi, A.K. Kasi, Performance analysis of passive optical networks with energy saving through the integrated sleep mode, Opt. Switch. Netw. 21 (2016) 16–30.
[85] A. Dixit, B. Lannoo, D. Colle, M. Pickavet, P. Demeester, Energy efficient dynamic bandwidth allocation for Ethernet passive optical networks: overview, challenges, and solutions, Opt. Switch. Netw. 18 (Part 2) (2015) 169–179.
[86] O. Brun, J.-M. Garcia, Analytical solutions of finite capacity M/D/1 queues, J. Appl. Prob. 11 (2000) 1092–1098.
[87] H. Tijms, New and old results for the M/D/c queue, Int. J. Electron. Commun. 60 (2) (2006) 125–130.

Po-Yen Chen received the Ph.D. degree in electrical engineering from Arizona State University, Tempe, USA, in 2015. He currently works as an advanced product development researcher in Taiwan. His research interests include performance analysis and modeling of wireless communication systems and hybrid wireless mesh networks.

Martin Reisslein is a Professor in the School of Electrical, Computer, and Energy Engineering at Arizona State University (ASU), Tempe, USA. He received the Ph.D. in systems engineering from the University of Pennsylvania, Philadelphia, PA, in 1998. He currently serves as Associate Editor for the IEEE Transactions on Mobile Computing, the IEEE Transactions on Education, and IEEE Access as well as Computer Networks and Optical Switching and Networking. He is Associate Editor-in-Chief for the IEEE Communications Surveys & Tutorials and chairs the steering committee of the IEEE Transactions on Multimedia.